https://dx.doi.org/10.1016/j.jorganchem.2023.122827

Aqueous Supramolecular Assemblies of Luminescent Cyclometalated Gold (III) Amphiphiles with Biocompatibility

Ming-Hin Chau,[a,c] Aries Kwok-Heung Chan,[a,c] Yikun Ren,[a] Jia-Jun Jiang,[a] Man-Kin Wong,[a,b] and Franco King-Chi Leung*,[a]

[a] State Key Laboratory of Chemical Biology and Drug Discovery, Department of Applied Biology and Chemical Technology, The Hong Kong Polytechnic University, Hong Kong, China.

[b] Department of Food Science and Nutrition, The Hong Kong Polytechnic University, Hong Kong, China.

[c] These authors contributed equally to this work.

* Corresponding Author: kingchifranco.leung@polyu.edu.hk (F.K.-C. Leung)

KEYWORDS: *Supramolecular Assembly, Cyclometalated Gold (III) Complex, Gold Amphiphile, Biocompatible, Supramolecular Nanostructure*

Abstract:

Gold (III) complex-based amphiphiles in aqueous media have recently been demonstrated with high structural sensitivity to external stimulations, enabling new prospect for soft functional material applications. Here we demonstrate an advanced supramolecular assembly system of gold (III) amphiphiles reversibly controlled by counterions exchange. More importantly, the luminescent properties of the gold (III) amphiphiles are enhanced by implementation of σ-donating mono-alkynyl

ligand. Gold (III) amphiphiles demonstrate with good cytocompatibilities to human bone marrow-derived mesenchymal stem cells.

1. Introduction

Supramolecular assemblies are commonly found in biological systems to serve vital roles in proper biological functions [1–3]. Synthetic supramolecular assemblies, as an alternative strategy to its natural counterpart, provide structural versatility and advanced functions in response to non-biocompatible external stimulations [4–7], *e.g.*, UV-light, pH, etc [8–10]. Amphiphile, featured with a combination of hydrophilic and hydrophobic motifs, is a class of common synthetic organic molecular designs in enabling tunable functions and potential aqueous solubility [11]. Organic amphiphiles in aqueous media, such as chromophore-based [12–15], amino acid-based, and photoresponsive molecular amphiphiles [4,16], have been extensively investigated in past few decades. Metal-ligand amphiphiles have been demonstrated as a promising alternative strategy to organic amphiphiles, due to the structural diversity and versatility of ligand modifications [17–21]. Fine adjustment of metal-ligand amphiphile design enables controls of supramolecular interactions and its resulting supramolecular nanostructures [17,21].

Gold (I) and gold (III) complexes, featured with excellent luminescent properties and aqueous stability, have been developed for applications in catalysis [22–26], bioconjugation methods [27–32], and optoelectronic materials [33,34]. Gold complexes-based amphiphiles was firstly reported by Che and co-workers [35], in using of cyclometalated gold (III) complexes linked to polyethylene glycol (PEG) chain for improved aqueous solubility. Namely, the gold (III) amphiphiles form micellar nanostructures for *in-vitro* phototoxicity [35]. Kinetically controlled supramolecular assemblies of charged cyclometalated gold (III) amphiphiles in ACN/water media were reported by the same group [36]. Charged cyclometalated gold (III) amphiphiles were further demonstrated by Yam, showing

intrinsic multiple responsiveness and organic gel-sol processes [37]. It is noted that these reported cyclometalated gold (III) amphiphiles were highly sensitive to minor change of molecular structure and subsequently induced supramolecular structural transformations [35–37]. On the basis of these pioneering cyclometalated gold (III) amphiphile designs [38–42], we reported the first reversibly counterion controlled supramolecular assembly transformations of cyclometalated gold (III) amphiphiles in aqueous media [43]. However, the luminescent properties and cytocompatibilities of this reversibly counterion controlled supramolecular assembly system remain unexplored.

Pioneered by Yam, cyclometalated gold (III) alkynyl complexes have been demonstrated extensively with enhanced ambident luminescent properties, due to the strong σ-donating alkynyl ligands rendering the metal center more electron rich [37,44]. Herein, we design and synthesize a new series of cyclometalated gold (III) amphiphiles (GA) with enhanced luminescent properties in aqueous media and biocompatibility. Cyclometalated gold (III) complex core is connected to a quaternary ammonium ion with an alkyl-linker, inducing molecular phase separation for improved aqueous solubility. Strong σ-donating alkynyl ligands are directly bonded to the cyclometalated gold (III) complex core, enabling ambident luminescence of GAs. Large aspect ratio of supramolecular nanostructures is formed upon dissolution of GAs into aqueous media. The packing parameters of GAs can be tuned reversibly by counterions. Cytocompatibilities of GAs in aqueous media has been clearly demonstrated with limited cytotoxicity at low concentration of GAs. By elucidating conditions of supramolecular assembling processes, luminescent properties, and cytocompatibilities of GAs, it could open up new prospects toward fabrications of stimuli-controlled supramolecular soft functional materials.

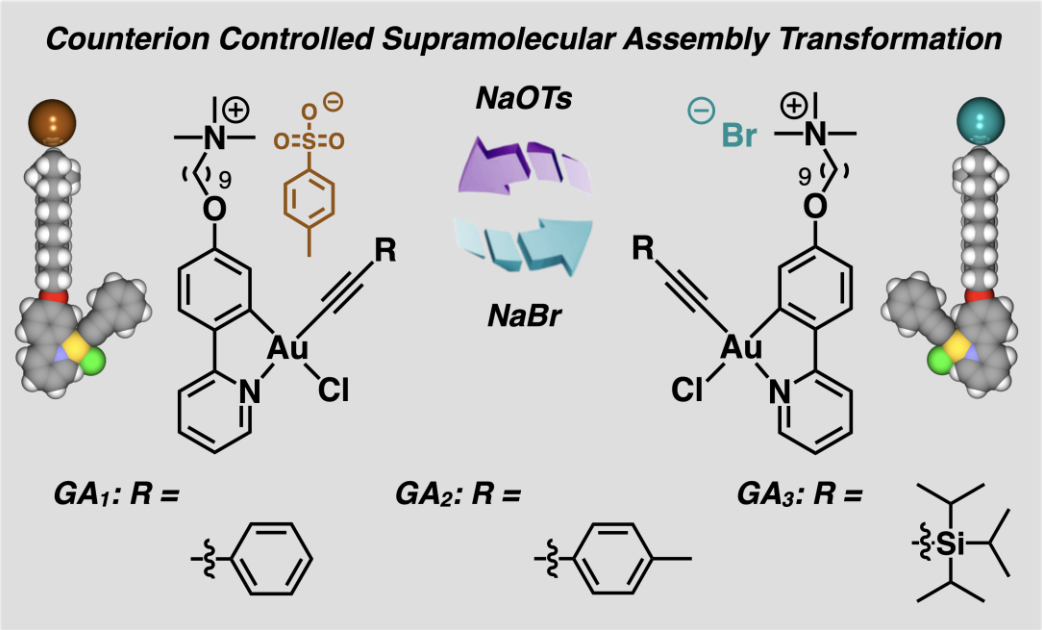

Scheme 1. Schematic illustration of the design of cyclometalated gold (III) amphiphiles.

2. Materials and methods

2.1. Materials

All commercial reagents are purchased from Acros Organics, Sigma Aldrich and Tokyo Chemical Industry Co. Ltd, and were used as received unless otherwise specified. All reactions were performed under nitrogen unless otherwise specified. Analytical thin layer chromatography (TLC) was performed with Macherey-Nagel Silica gel 60 UV254 aluminium plates and visualization was accomplished by UV light (254 / 365 nm) or staining with phosphomolybdic acid followed by heating. Flash column chromatography was performed using Macherey-Nagel Silica gel 60 (230–400 mesh). Deuterated solvents were purchased from Cambridge Isotope Laboratories Inc.

2.3. UV-vis Spectroscopy

UV-vis measurements were performed on Agilent Cary 60 UV-Visible Spectrophotometer with a 1 cm path length quartz cuvette. A Luma 40/8453 temperature-controlled cuvette holder with four optical ports was mounted in the sample compartment of Agilent Cary 60 UV-Visible Spectrophotometer. Measurement of all samples were carried out at 20 °C.

2.4. Preparation of aqueous sample

GAs (1 wt.%) was dissolved in fresh deionized water (DI water). The solution was heated at 50 °C for 5 min, then slowly cooled to 20 °C at a rate of 1.0 °C/min to form assembled structure. For TEM study, the annealed solution was further diluted to 0.2 wt.%.

2.5. Transmission Electron Microscopy (TEM)

TEM was performed on a JEOL Model JEM-2010 Transmission Electron Microscope with hair pin type tungsten filament operating at 120 kV equipped with Gatan 794 CCD camera. TEM sample were prepared by depositing sample solutions (5.0 μL) onto a carbon grid (Micro to Nano, EMR Carbon support film on copper, 400 square mesh) for 20 s. The sample solution was removed by blotting and UranyLess EM stain solution (Electron Microscopy Science, 5.0 μL) was directly deposited onto the grid for 20 s and the stain was removed by blotting.

2.6. Dynamic Light Scattering (DLS)

Dynamic Light Scattering intensities of each sample were measured on a Wyatt Technology DynaPro NanoStar. The scattering intensities were recorded as a parameter for assembly size, given that the objects in solution are anisotropic and the models used by Wyatt software are fitting for spherical objects. According to previously described procedures [12], the critical aggregation concentration

(CAC) of **GAs** is determined by the scattering intensities of the solutions of **GAs** (concentration: 1.0 × 10^{-3} to 1.0 mM) at 20 °C. The scattering rate was normalized by the concentration of the solution to yield the molar scattering intensity (M Counts s^{-1} m^{-1}). Ten replications were performed, and the data was averaged to show the molar scattering intensity and corresponding standard deviation.

2.7 Fluorescence

Fluorescence measurements were performed on an Agilent G9800AA Cary Eclipse fluorescence spectrophotometer with a 1 cm path length quartz cuvette. All measurements were carried out at room temperature.

2.8 Cytotoxicity test

The cytotoxicity of GAs were characterized by 3-(4,5-dimethylthiazol-2-yl)-5-(3-carboxymethoxyphenyl)-2-(4-sulfophenyl)-2H-tetrazolium (MTS) assay. Human bone-marrow Mesenchymal Stem Cells (hBM-MSCs) were seeded in 96-well plate as a density of 3000 cells per well. After incubated in growth media which contains Minimum Essential Medium (MEM Alpha, no phenol red, Gibco, USA), 10% Fetal Bovine Serum (FBS, Gibco, USA) and 1% Antibiotic-Antimycotic (Gibco, USA) for 12 h, different concentration of GAs was added and incubated with cells for 24 h, respectively. For MTS assay, MTS solution was added to each well and incubated for 2 h at 37 °C and 5% CO_2. The absorbance of each well was measured at 490 nm using LEDETECT 96 microplate reader.

3. RESULT AND DISCUSSION

3.1. Design and Synthesis of GAs

GAs were designed with cyclometalated gold (III) complex core, functionalized with a σ-donating alkynyl ligand, attached with a quaternary ammonium ion motif with a nonyl-linker with a tosylate counterion (Scheme 1). It is noted that extended conjugated system decrease aqueous solubilities of the resulting supramolecular assemblies, hence, mono-alkynyl ligand is employed in this current design. The general synthetic route for gold (III) amphiphiles **GA$_1$**, **GA$_2$**, and **GA$_3$** is shown in supporting infomation. According to previously reported procedure [45–48], GA precursor **1** can be obtained and purified in a satisfactory isolated yield. Dichloro-gold (III) complex core of **1** was added with alkynes **2** in the presence of triethylamine and catalytic amount of copper iodide, affording GAs with a mono-alkynyl ligand in modest yields (29–46%) after multiple column purifications. The chemical structures of newly prepared gold (III) amphiphiles **GA$_1$**, **GA$_2$**, and **GA$_3$** were characterized unambiguously using ^{1}H, ^{13}C NMR and high-resolution mass spectrometry (Figures S11–S15).

*3.2. Luminescent Properties and Counterion Controlled Supramolecular Assemblies Transformations of **GA$_1$***

A freshly prepared aqueous solution of **GA$_1$** (11.6 mM, 1.0 weight%) was heated to 50 °C and slowly cooled to 20 °C at a rate of 1.0 °C/min, *i.e.*, thermal annealing process. The aqueous solution was diluted into a range of concentrations from 0.01 to 1.0 mM for the determination of the critical aggregation concentration (CAC) by using a dynamic light scattering (DLS). The CAC of **GA$_1$** was determined as 50 mM (Figure S1). An aqueous solution of **GA$_1$** (400 μM) was heated to 50 °C and slowly cooled to 20 °C at a rate of 1.0 °C/min, studied by UV-vis absorption spectroscopy (Figure 1a). The absorption maximum at 355 nm of **GA$_1$** increased in the cooling process with a formation of bathochromic-shifted shoulder band appearing at ~450 nm (Figure 1a, red-line). Though higher

concentration of **GA$_1$** was required (1.0 mM) for adequate luminescence, an emission band at 470–600 nm was observed, which was excited by 360 nm (Figures 1b). The vibronic structured emission band originates from the intra-ligand excited state of the cyclometalated ligand. [37, 39–41, 44, 47–48]. Additionally, **GA$_1$** was dissolved in dichloromethane/methanol (1:1 volume ratio) to give an absorption band at 300–390 nm with absorption maximum at 355 nm (Figure S2a). Using the identical solvent system, **GA$_1$** (1.0 mM) gives much lower intensity emission band at 420–600 nm (Figure S2b) than that of **GA$_1$** in aqueous media (Figure 1b). Given that GA precursor **1** in aqueous media showed limited luminescent properties even at high concentration (Figure S3), the results indicated that implementation of strong a σ-donating alkynyl ligand to the cyclometalated gold (III) complex core can enhance the luminescent properties of **GA$_1$** in aqueous media.

A thermal annealed aqueous solution of **GA$_1$** (2.32 mM) was examined with negative-stained transmission electron microscopy (TEM), revealing supramolecular nanofibers with hundreds of nanometres to micrometres in length and ~ 9 nm in diameter (Figure 1c). The supramolecular nanostructures of aqueous solution of **GA$_1$** are highly similar to that of observed in GA precursor **1** as reported previously, except the diameter of the supramolecular nanofibers increased in **GA$_1$**. Thermal annealed supramolecular nanofibers of **GA$_1$** (400 μM, final concentration) was added with aqueous solution of sodium bromide (2.0 equiv.) and subsequently heated to 50 °C and slowly cooled to 20 °C at a rate of 1.0 °C/min. The absorption spectrum of the obtained solution shown absorption maximum at 355 nm was significantly reduced with a shoulder band at 400–500 nm formed (Figure 1d). An aqueous solution of **GA$_1$** (1.0 mM), prepared from the identical method in the presence of sodium bromide, shows an emission band at 400–600 nm (Figure 1e) with significant reduced intensity than that of observed in Figure 1b. The results indicated that counterion exchange from tosylate to bromide induces increasement of packing parameters of **GA$_1$** and subsequently changes the packing structure from less organized nanofibers to well-organized nanotubes. In this connection, luminescent property of **GA$_1$** was partially quenched with the increased aggregation in the resulting well-organized nanotubular structures. The TEM image of the solution **GA$_1$** (2.32 mM), prepared

from above method, revealed entangled nanotubular nanostructures with outer diameter ~19 nm in the presence of sodium bromide (Figure 1f). Counterion controlled supramolecular transformation of **GA$_1$** is clearly demonstrated, more importantly, it provides as a control of luminescent properties of **GA$_1$** by simply counterion bromide addition. Furthermore, the nanotubes of **GA$_1$** were subsequently reformed after addition of sodium tosylate (2.0 equiv.) as further counterion exchange (Figure S4), showing partial supramolecular transformation of nanotubes to nanofibers with a mixture of irregular aggregates. Incomplete supramolecular transformation of **GA$_1$** is possibly attributed to the increased ion strength after a series of sodium salts additions.

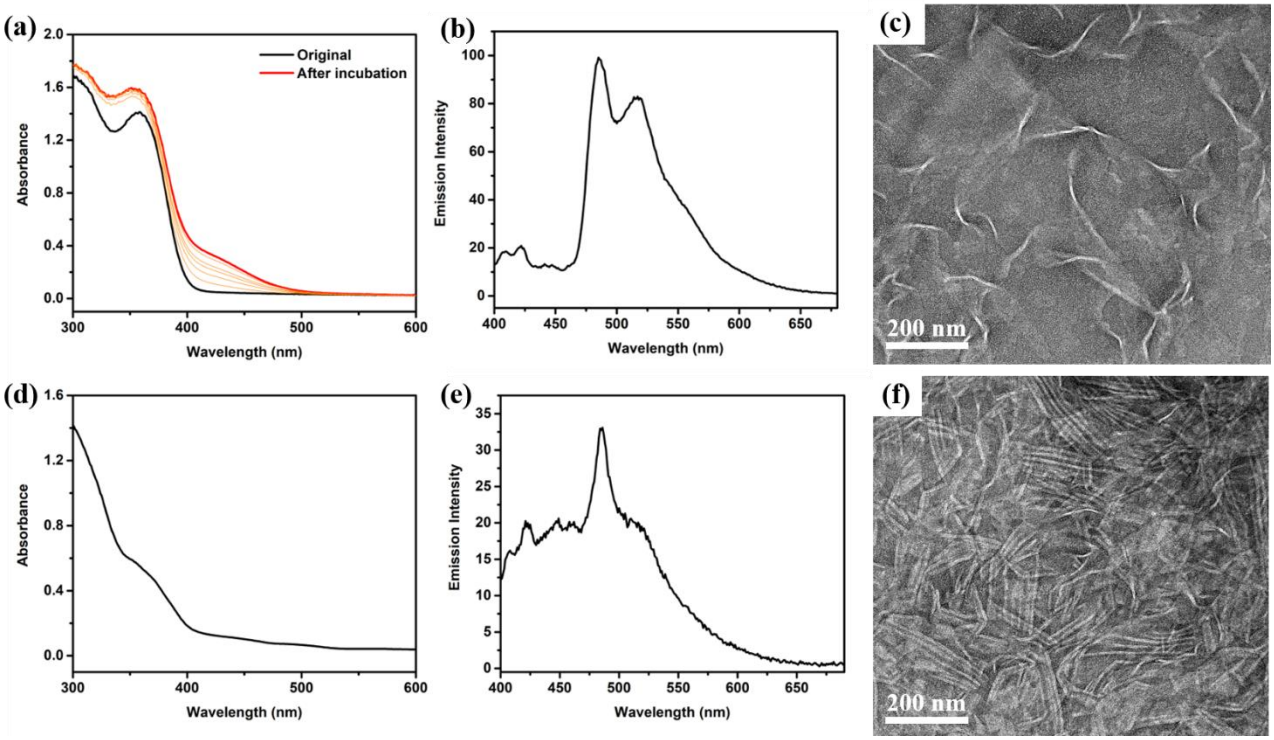

Fig. 1. (a) UV-vis absorption spectra of **GA$_1$** (400 μM) in DI water before (black-line) and after incubation, (red-line). (b) Emission spectum of compound **GA$_1$** (1 mM) in DI water. (c) TEM image of thermal annealed solution of **GA$_1$** (2.32 mM). (d) UV-vis absorption spectrum of **GA$_1$** (400 μM) in DI water after addition of bromide counterion. (e) Emission spectrum of compound **GA$_1$** (1 mM) in DI water after addition of bromide counterion. (f) TEM image of thermal annealed solution of **GA$_1$** after addition of bromide counterion (2.32 mM).

3.3. Luminescent Properties and Supramolecular Assemblies of Structurally Derived GAs

GA2, a structurally derived GAs implemented with a 4-methylphenylacetylene ligand, was prepared according to the similar procedure, affording mono-alkynyl **GA2**. **GA2** was dissolved in organic media dichloromethane/methanol (1:1) to show strong absorption band at 320–390 nm with an absorption maximum at 356 nm (Figure S5a), while the identical solution shows luminescent properties with emission band at 450–550 nm (Figure S5b). In contrast, an aqueous solution of **GA2**, thermally annealed at 50 °C and slowly cooled to 20 °C at a rate of 1.0 °C/min, showed enhanced absorption band at 320–500 nm (Figure 2a). Notably, the luminescent intensity of an aqueous solution of **GA2** (1.0 mM) was reduced, possibly due to subtle change of packing structure with slightly increased steric hindrance of the alkynyl ligand. A pair of emission maxima were observed at 470 nm and 530 nm (Figure 2b), indicating aggregated GA can show blue-green color emission upon 320 nm excitation. Similar to **GA1**, the vibronic structured emission band was also observed. The CAC of **GA2** was determined as 50 mM (Figure S6). A thermally annealed aqueous solution of **GA2** (2.28 mM) was imaged under TEM (Figure 2c), revealing nanofibers structure with diameter ~ 6 nm essentially identical to that of observed in GA precursor **1** in aqueous media. Thermal annealed supramolecular nanofibers of **GA2** (2.28 μM, final concentration) was added with aqueous solution of sodium bromide (2.0 equiv.) and subsequently heated to 50 °C and slowly cooled to 20 °C at a rate of 1.0 °C/min. Nanofibers were transformed into a mixture of bundled nanofibers with vesicles (Figure S7), indicating supramolecular transformation of **GA2** could be controlled by counterion addition.

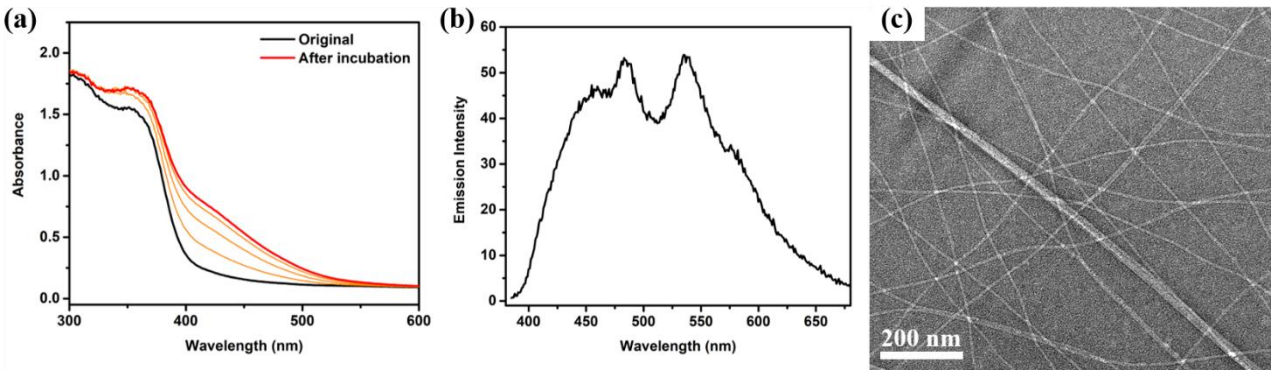

Fig. 2. (a) UV-vis absorption spectra of **GA2** (400 μM) in DI water before (black-line) and after

incubation, (red-line). (b) Emission spectrum of compound **GA$_2$** (1 mM) in DI water. (c) TEM image of thermal annealed solution of **GA$_2$** (2.28 mM).

Given that cyclometalated gold (III) complex implemented with (triisopropylsilyl)acetylene ligands enhance its luminescent properties [47], **GA$_3$** was prepared from the identical synthetic method with (triisopropylsilyl)acetylene ligands, giving a mixture of mono-alkynyl GA (**GA$_3$**) and di-alkynyl GA (**GA$_3$**') of **GA$_3$** in a ratio of 1:5 (Figure S8). It is noted that multiple column chromatography separations have been performed but mono-alkynyl **GA$_3$** could not be further purified from di-alkynyl **GA$_3$**'. Absorption spectra of **GA$_3$** in both organic (Figure S9a) and aqueous (Figure S9b) are essentially identical to that of observed in **GA$_1$** (Figure 1a). At 1.0 mM of mixture of **GA$_3$** in aqueous media, minor light scattering was observed, possibly due to reduced aqueous solubility in the presence of higher ratio of di-alkynyl **GA$_3$**'. Significant enhanced luminescent properties of **GA$_3$** (1.0 mM) in aqueous media were observed along with an emission band at 350–550 nm (λ_{max} = 420 nm) (Figure 3a), possibly due to high ratio of di-alkynyl **GA$_3$**'. Similar enhanced luminescent intensity of **GA$_3$** (1.0 mM) in DCM/MeOH (1:1 volume ratio) was observed (Figure S9c). The CAC of **GA$_3$** was determined as 20 mM (Figure S10). A thermal annealed aqueous solution of **GA$_3$** (1.97 mM) was imaged TEM to show a mixture of supramolecular nanosheet-like structures and solid particles with hundreds of nanometers in diameter (Figure 3b). Nanosheet-like structures of **GA$_3$** is potentially constructed from the mono-alkynyl **GA$_3$**, while solid particles should be originated from the low aqueous solubility di-alkynyl **GA$_3$**'. Although the complications of resulting supramolecular assemblies of **GA$_3$** remained challenging in study of the supramolecular transformations, the results indicated the structural modifications, attaching σ-donating alkynyl ligand to the cyclometalated gold (III) complex core, can improve the luminescent properties in the resulting supramolecular assemblies.

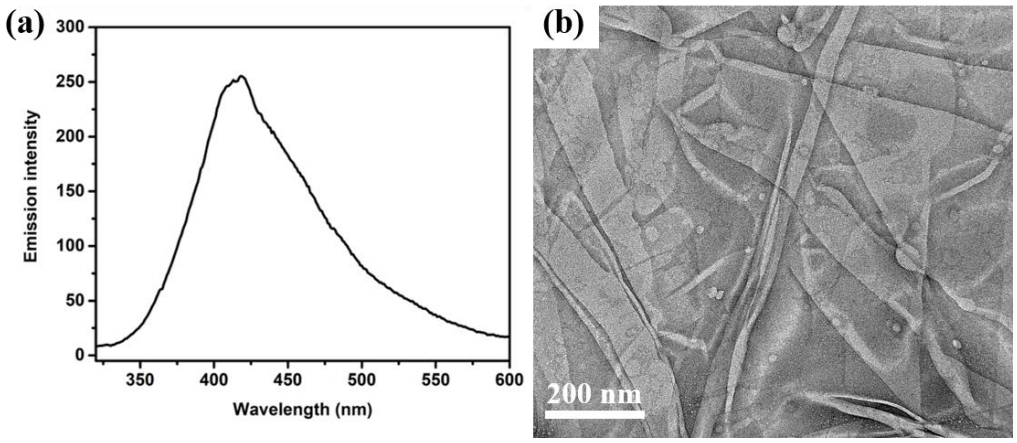

Fig. 3. (a) Emission spectrum of compound **GA$_3$** (1 mM) in DI water. (b) TEM image of thermal annealed solution of **GA$_3$** (1.97 mM).

3.4. Cytocompatibility of GAs

Aqueous solutions of **GA$_1$**, **GA$_2$**, and GA precursor **1** were prepared after thermal annealing process and subjected for cytocompatibility studies, except **GA$_3$** due to its lower aqueous solubility. An MTS mitochondrial activity assay was employed for determining cell viability of human bone marrow-derived mesenchymal stem cells (hBM-MSCs) in the presence of aqueous solution of GA precursor **1** in concentration range of 40–100 μM (Figure 4a). In Figure 4a, the results were normalized to viability of hBM-MSCs in the absence of GAs. High cell viabilities (~90%) of hBM-MSCs over 24 h of culture with the solution of GA precursor **1** in concentration range of 40–100 μM. According to identical method, the cell viability of **GA$_1$** was investigated (Figure 4b), showing increased cytotoxicity over 60 μM of **GA$_1$**. **GA$_2$** showed reduced cytotoxicity to hBM-MSCs upon incubation in concentration range of 40–100 μM (Figure 4c). In considering the nanostructures of GAs, GA precursor **1** and **GA$_2$** showed essentially identical nanofibers, while the nanofibers of **GA$_1$**

are larger in diameter. The results indicated a plausible dependence between the cytotoxicity of GAs and the resulting nanostructures of GAs.

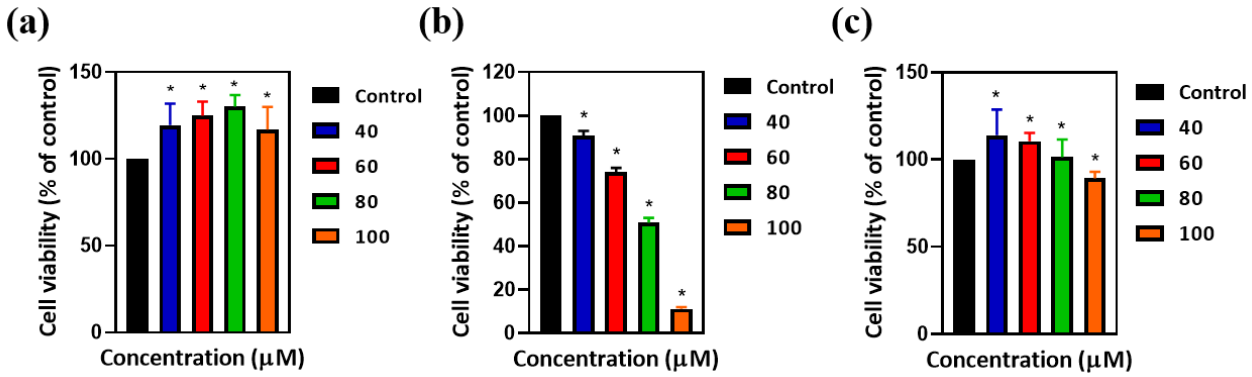

Fig. 4. (a) hBM-MSCs viability after incubated with (a) GA precursor **1**, (b) **GA$_1$** and (c) **GA$_2$** gradient solutions for 24 h, respectively. All values are mean ± standard deviation of n = 3. * denotes $P < 0.05$, which represents for statistically difference compared to the control group.

4. CONCLUSION

Gold (III) amphiphiles, functionalized with σ-donating mono-alkynyl ligands, were designed to show enhanced luminescent properties in both organic and aqueous media. Nanofibers of **GA$_1$** and **GA$_2$** were confirmed with TEM and shown CAC below 50 μM by DLS. Upon addition of NaBr, counterion exchanges enable supramolecular assembly transformations of **GA$_1$** from nanofibers to nanotubes, which is reversible upon further NaOTs counterion addition. Cytocompatibilities of **GA$_1$**, **GA$_2$**, and GA precursor **1** were clearly shown that supramolecular assemblies of GAs have limited cytotoxicity to the hBM-MSCs. The current approach would open up new generations of multi-functional supramolecular assembly of gold (III) amphiphiles.

Author Contributions

M.-H. Chau performed all the assembly characterizations for GAs in this work, while A. K.-H. Chan performed all organic synthesis and characterizations. Y. Ren carried out all cytotoxicity study. J. J.

Jiang performed preliminary study of GAs. M. K. Wong commented on the GA work. F. K.-C. Leung co-wrote, conceived and supervised the research. All authors discussed the results and commented on the manuscript.

Conflicts of interest

There are no conflicts to declare.

Acknowledgements

This work was supported financially by the Croucher Foundation (Croucher Innovation Award-2021 to F.K.C.L.), the Hong Kong Research Grant Council (GRF 15305822 to F.K.C.L.), (GRF 15300019 and 15300520 to M.K.W.), and The Hong Kong Polytechnic University (W08A, ZVST). We acknowledge the technical support from UCEA and ULS of PolyU.

References

[1] N.S. Simmons, E.R. Blout, The Structure of Tobacco Mosaic Virus and Its Components: Ultraviolet Optical Rotatory Dispersion, Biophys. J. 1 (1960) 55–62. https://doi.org/10.1016/S0006-3495(60)86875-0.

[2] T. Lino, Assembly of Salmonella Flagellin in Vitro and in Vivo, J. Supramol. Struct. 2 (1974) 372-384. https://doi.org/10.1002/jss.400020226.

[3] D. Chapman, Phase transitions and fluidity characteristics of lipids and cell membranes, Q. Rev. Biophys. 8 (1975) 185–235. https://doi.org/10.1017/S0033583500001797.

[4] S. Chen, R. Costil, F.K.-C. Leung, B.L. Feringa, Self-Assembly of Photoresponsive Molecular Amphiphiles in Aqueous Media, Angew. Chem. Int. Ed. 60 (2021) 11604–11627. https://doi.org/10.1002/anie.202007693.

[5] B.L. Feringa, The Art of Building Small: From Molecular Switches to Motors (Nobel Lecture), Angew. Chem. Int. Ed. 56 (2017) 11060–11078. https://doi.org/10.1002/anie.201702979.

[6] E. Krieg, M.M.C. Bastings, P. Besenius, B. Rybtchinski, Supramolecular polymers in aqueous media, Chem. Rev. 116 (2016) 2414–2477. https://doi.org/10.1021/acs.chemrev.5b00369.

[7] T. Aida, E.W. Meijer, S.I. Stupp, Functional Supramolecular Polymers, Science 335 (2012) 813–817. https://doi.org/10.1126/science.1205962.

[8] D. Dattler, G. Fuks, J. Heiser, E. Moulin, A. Perrot, X. Yao, N. Giuseppone, Design of Collective Motions from Synthetic Molecular Switches, Rotors, and Motors, Chem. Rev. 120 (2020) 310–433. https://doi.org/10.1021/acs.chemrev.9b00288.

[9] M. Baroncini, S. Silvi, A. Credi, Photo- And Redox-Driven Artificial Molecular Motors, Chem. Rev. 120 (2020) 200–268. https://doi.org/10.1021/acs.chemrev.9b00291.

[10] H. Shigemitsu, T. Fujisaku, W. Tanaka, R. Kubota, S. Minami, K. Urayama, I. Hamachi, An adaptive supramolecular hydrogel comprising self-sorting double nanofibre networks, Nat. Nanotechnol. 13 (2018) 165–172. https://doi.org/10.1038/s41565-017-0026-6.

[11] J. Volarić, W. Szymanski, N.A. Simeth, B.L. Feringa, Molecular photoswitches in aqueous environments, Chem. Soc. Rev. 50 (2021) 12377–12449. https://doi.org/10.1039/d0cs00547a.

[12] M.-H. Chau, M.C.A. Stuart, F.K.-C. Leung, Red-light driven photoisomerisation and supramolecular transformation of indigo amphiphiles in aqueous media, Colloids Surf. A Physicochem. Eng. Asp. 661 (2023) 130939. https://doi.org/10.1016/j.colsurfa.2023.130939.

[13] L.-H. Cheung, T. Kajitani, F.K.-C. Leung, Visible-light controlled supramolecular transformations of donor-acceptor Stenhouse adducts amphiphiles at multiple length-scale, J. Colloid Interface Sci. 628 (2022) 984–993. https://doi.org/10.1016/j.jcis.2022.08.034.

[14] A.K.-H. Chau, L.-H. Cheung, F.K.-C. Leung, Red-light controlled supramolecular co-assembly transformations of stiff stilbene and donor acceptor stenhouse adduct amphiphiles, Dyes Pigm. 208 (2022) 110807. https://doi.org/10.1016/j.dyepig.2022.110807.

[15] K.S.-Y. Kwan, Y.-Y. Lui, T. Kajitani, F.K.-C. Leung, Aqueous Supramolecular Co-Assembly of Anionic and Cationic Photoresponsive Stiff- Stilbene Amphiphiles, Macromol. Rapid Commun. (2022) 2200438. https://doi.org/10.1002/marc.202200438.

[16] A.K.-H. Chau, F.K.-C. Leung, Exploration of molecular machines in supramolecular soft robotic systems, Adv. Colloid Interface Sci. 315 (2023) 102892. https://doi.org/10.1016/j.cis.2023.102892.

[17] J.K.-L. Poon, Z. Chen, S.Y.-L. Leung, M.-Y. Leung, V.W.-W. Yam, Geometrical manipulation of complex supramolecular tessellations by hierarchical assembly of amphiphilic platinum (II) complexes, Proc. Natl. Acad. Sci. 118 (2021). https://doi.org/10.1073/pnas.2022829118.

[18] V.W.-W. Yam, A.S. Law, Recent advances in supramolecular self- assembly and biological applications of luminescent alkynylplatinum (II) polypyridine complexes, J. Chin. Chem. Soc. 67 (2020) 2246–2252. https://doi.org/10.1002/jccs.202000536.

[19] H.L.-K. Fu, V.W.-W. Yam, Supramolecular Metallogels of Platinum (II) and Gold (III) Complexes, Chem. Lett. 47 (2018) 605–610. https://doi.org/10.1246/cl.180096.

[20] T. Owen, A. Butler, Metallosurfactants of bioinorganic interest: Coordination-induced self assembly, Coord. Chem. Rev. 255 (2011) 678–687. https://doi.org/10.1016/j.ccr.2010.12.009.

[21] M.J. Mayoral Muñoz, G. Fernández, Metallosupramolecular amphiphilic π-systems, Chem. Sci. 3 (2012) 1395. https://doi.org/10.1039/c2sc01101h.

[22] W. Zi, F. Dean Toste, Recent advances in enantioselective gold catalysis, Chem. Soc. Rev. 45 (2016) 4567–4589. https://doi.org/10.1039/C5CS00929D.

[23] J.-J. Jiang, M.-K. Wong, Recent Advances in the Development of Chiral Gold Complexes for Catalytic Asymmetric Catalysis, Chem. Asian J. 16 (2021) 364–377. https://doi.org/10.1002/asia.202001375.

[24] L. Rocchigiani, M. Bochmann, Recent Advances in Gold (III) Chemistry: Structure, Bonding, Reactivity, and Role in Homogeneous Catalysis, Chem. Rev. 121 (2021) 8364–8451. https://doi.org/10.1021/acs.chemrev.0c00552.

[25] J.-J. Jiang, J.-F. Cui, B. Yang, Y. Ning, N.C.-H. Lai, M.-K. Wong, Chiral Cyclometalated Oxazoline Gold (III) Complex-Catalyzed Asymmetric Carboalkoxylation of Alkynes, Org. Lett. 21 (2019) 6289–6294. https://doi.org/10.1021/acs.orglett.9b02171.

[26] J.-F. Cui, H.-M. Ko, K.-P. Shing, J.-R. Deng, N.C.-H. Lai, M.-K. Wong, C, O-Chelated BINOL/Gold (III) Complexes: Synthesis and Catalysis with Tunable Product Profiles, Angew. Chem. Int. Ed. 56 (2017) 3074–3079. https://doi.org/10.1002/anie.201612243.

[27] P. Destito, C. Vidal, F. López, J.L. Mascareñas, Transition Metal- Promoted Reactions in Aqueous Media and Biological Settings, Chem. Eur. J. 27 (2021) 4789–4816. https://doi.org/10.1002/chem.202003927.

[28] S.R. Thomas, A. Casini, Gold compounds for catalysis and metal-mediated transformations in biological systems, Curr. Opin. Chem. Biol. 55 (2020) 103–110. https://doi.org/10.1016/j.cbpa.2019.12.007.

[29] T.-C. Chang, K. Tanaka, In vivo organic synthesis by metal catalysts, Bioorg. Med. Chem. 46 (2021) 116353. https://doi.org/10.1016/j.bmc.2021.116353.

[30] H.-Y. Sit, B. Yang, K. K.- Y. Kung, J. S.- L. Tam, M.-K. Wong, Fluorescent Labelling of Glycans with FRET- Based Probes in a Gold (III)- Mediated Three- Component Coupling Reaction, ChemPlusChem. 84 (2019) 1739–1743. https://doi.org/10.1002/cplu.201900612.

[31] K.K.-Y. Kung, H.-M. Ko, J.-F. Cui, H.-C. Chong, Y.-C. Leung, M.-K. Wong, Cyclometalated gold (III) complexes for chemoselective cysteine modification via ligand controlled C–S bond-forming reductive elimination, Chem. Commun. 50 (2014) 11899–11902. https://doi.org/10.1039/C4CC04467C.

[32] H.-M. Ko, J.-R. Deng, J.-F. Cui, K.K.-Y. Kung, Y.-C. Leung, M.-K. Wong, Selective modification of alkyne-linked peptides and proteins by cyclometalated gold (III) (C^N) complex-mediated alkynylation, Bioorg. Med. Chem. 28 (2020) 115375. https://doi.org/10.1016/j.bmc.2020.115375.

[33] V.W.-W. Yam, V.K.-M. Au, S.Y.-L. Leung, Light-Emitting Self-Assembled Materials Based on d^8 and d^{10} Transition Metal Complexes, Chem. Rev. 115 (2015) 7589–7728. https://doi.org/10.1021/acs.chemrev.5b00074.

[34] V.W.-W. Yam, A.K.-W. Chan, E.Y.-H. Hong, Charge-transfer processes in metal complexes enable luminescence and memory functions, Nat. Rev. Chem. 4 (2020) 528–541. https://doi.org/10.1038/s41570-020-0199-7.

[35] F. Wang, M. Lan, W.-P. To, K. Li, C.-N. Lok, P. Wang, C.-M. Che, A macromolecular cyclometalated gold (III) amphiphile displays long-lived emissive excited state in water: self-

assembly and in vitro photo-toxicity, Chem. Commun. 52 (2016) 13273–13276. https://doi.org/10.1039/C6CC06767K.

[36] Q. Wan, J. Xia, W. Lu, J. Yang, C.-M. Che, Kinetically Controlled Self-Assembly of Phosphorescent Au ^{III} Aggregates and Ligand-to-Metal–Metal Charge Transfer Excited State: A Combined Spectroscopic and DFT/TDDFT Study, J. Am. Chem. Soc. 141 (2019) 11572–11582. https://doi.org/10.1021/jacs.9b04007.

[37] M.-Y. Leung, S.Y.-L. Leung, K.-C. Yim, A.K.-W. Chan, M. Ng, V.W.-W. Yam, Multiresponsive Luminescent Cationic Cyclometalated Gold (III) Amphiphiles and Their Supramolecular Assembly, J. Am. Chem. Soc. 141 (2019) 19466–19478. https://doi.org/10.1021/jacs.9b10607.

[38] J.-J. Zhang, W. Lu, R.W.-Y. Sun, C.-M. Che, Organogold (III) Supramolecular Polymers for Anticancer Treatment, Angew. Chem. Int. Ed. 51 (2012) 4882–4886. https://doi.org/10.1002/anie.201108466.

[39] V.K.-M. Au, N. Zhu, V.W.-W. Yam, Luminescent Metallogels of Bis-Cyclometalated Alkynylgold(III) Complexes, Inorg. Chem. 52 (2013) 558–567. https://doi.org/10.1021/ic3007519.

[40] K.-C. Yim, V.K.-M. Au, L.-L. Hung, K.M.-C. Wong, V.W.-W. Yam, Luminescent Dinuclear Bis-Cyclometalated Gold (III) Alkynyls and Their Solvent-Dependent Morphologies through Supramolecular Self-Assembly, Chem. Eur. J. 22 (2016) 16258–16270. https://doi.org/10.1002/chem.201603186.

[41] S.K.-L. Siu, C. Po, K.-C. Yim, V.K.-M. Au, V.W.-W. Yam, Synthesis, characterization and spectroscopic studies of luminescent L-valine modified alkynyl-based cyclometalated gold (III) complexes with gelation properties driven by π–π stacking, hydrogen bonding and hydrophobic–hydrophobic interactions, CrystEngComm. 17 (2015) 8153–8162. https://doi.org/10.1039/C5CE01136A.

[42] K.-C. Yim, E.S.-H. Lam, K.M.-C. Wong, V.K.-M. Au, C.-C. Ko, W.H. Lam, V.W.-W. Yam, Synthesis, Characterization, Self-Assembly, Gelation, Morphology and Computational Studies of Alkynylgold (III) Complexes of 2,6-Bis(benzimidazol-2′-yl) pyridine Derivatives, Chem. Eur. J. 20 (2014) 9930–9939. https://doi.org/10.1002/chem.201402876.

[43] J.J. Jiang, A.K. Chau, M.-K. Wong, F.K.-C. Leung, Controlled Supramolecular Assembly of Gold (III) Amphiphiles in Aqueous Media, Eur. J. Inorg. Chem. 2022 (2022). e202200281. https://doi.org/10.1002/ejic.202200281.

[44] C.-H. Lee, M.-C. Tang, F.K.-W. Kong, W.-L. Cheung, M. Ng, M.-Y. Chan, V.W.-W. Yam, Isomeric Tetradentate Ligand-Containing Cyclometalated Gold (III) Complexes, J. Am. Chem. Soc. 142 (2020) 520–529. https://doi.org/10.1021/jacs.9b11587.

[45] E.C. Constable, T.A. Leese, Metal exchange in organomercury complexes; a facile route to cyclometallated transition metal complexes, J. Organomet. Chem. 335 (1987) 293–299. https://doi.org/10.1016/S0022-328X(00)99404-X.

[46] E.C. Constable, T.A. Leese, Cycloaurated derivatives of 2-phenylpyridine, J. Organomet. Chem. 363 (1989) 419–424. https://doi.org/10.1016/0022-328X(89)87129-3.

[47] J.A. Garg, O. Blacque, K. Venkatesan, Syntheses and Photophysical Properties of Luminescent Mono-cyclometalated Gold(III) *cis* -Dialkynyl Complexes, Inorg. Chem. 50 (2011) 5430–5441. https://doi.org/10.1021/ic102216v.

[48] V.K.-M. Au, K.M.-C. Wong, N. Zhu, and V.W.-W. Yam, Luminescent Cyclometalated Dialkynylgold(III) Complexes of 2-Phenylpyridine-Type Derivatives with Readily Tunable Emission Properties, Chem. Eur. J. 17 (2011) 130–142. https://doi.org/10.1002/chem.201001965.

Table of Content / Graphical Abstract